

A finite element study of masonry cracks

A.M. Fathy

Department of Properties of Materials, Faculty of Engineering, Ain Shams University, Cairo, Egypt

J. Planas

Departamento de Ciencia de Materiales, Universidad Politécnica de Madrid, Madrid, Spain

J.M. Sancho

Departamento de Ingeniería de Edificación, Escuela Politécnica Superior, Universidad CEU-San Pablo, Madrid, Spain

ABSTRACT: Brick walls of ceramic without any mortar covering or paint are used extensively in building façades in Spain. Their good appearance and high resistance to environmental attacks are the reasons of the widespread use of such walls in Spain. One of the most used masonry wall system is based on nonbearing panels hanging partially, about two thirds of the brick width, on the edge beams of the structural skeleton. The edge beam is veneered with special thinner bricks to achieve the visual continuity of the façade. A considerable number of these walls show cracking. In this work, finite element simulations were performed in order to gain insight on the causes of cracking. A special finite element, based on the strong discontinuity analysis and the cohesive crack theory is used in the numerical simulations. The results agree with the overall cracking patterns observed.

1 INTRODUCTION

Walls are the most used single masonry element. From a structural point of view, walls are classified as either load bearing or non-load bearing. To this latter category belong closures and partitions, fences, parapets, and exterior wythes of multi-wythe walls that are subjected mainly to horizontal loads perpendicular to the plane of the wall (Casabbone 1994).

Most masonry units available can be classified in one of the following groups: concrete block, solid concrete brick, clay block, clay brick (solid or cored), clay tile, sand lime units or adobe units (Yamin & Garcia 1994). Masonry bearing walls with reinforced concrete slabs is of large use in residential buildings up to five stories in U.S. and Latin American countries (Casabbone 1994, Meli & Garcia 1994, Garcia & Yamin 1994, Gallegos 1994). There are different masonry systems of this type of walls as unreinforced masonry, confined masonry or reinforced masonry. In the Latin American countries, masonry units, following the Spanish construction tradition, were mainly solid clay bricks and the walls were reinforced. The reinforcement was concentrated in the perimeter of the wall, embedded in concrete elements, giving birth to the system called confined masonry (Fig. 1).

Reinforced masonry system is applied to masonry walls strengthened with distributed reinforcement along its length and height (Fig. 2).

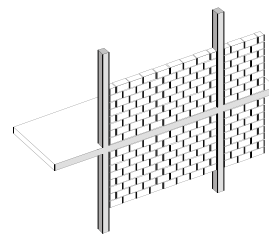


Figure 1: Confined masonry

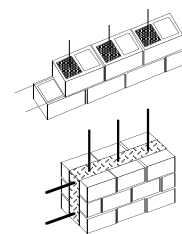


Figure 2: Reinforced masonry.

In the last decades, the price of residential flats raised considerably in Spain. One of the consequences was the reduction of the time employed in the building process. One of the most used construction systems for residential buildings is based on a skeleton of reinforced concrete or steel columns with reinforced concrete uni- or bidirectional slabs. Masonry walls are used as partitions. The façade is normally fabricated with double wythe wall with thermal insulation in between. The good quality and appearance of the ceramic masonry unit used lead to intensive use of this type of exterior walls without mortar cover or paint. The masonry wall can be built with totally or partially bearing over the end beams (Figs. 3 & 4). Also, the exterior wythe may be fabricated out of the plane, which contain the end beams. In this case, rigid steel angle is used to support the wall (Fig. 5)(Adell Argilés 2003). The edge beams in every floor are not in the same vertical plane. The horizontal eccentricities between those planes are in the same order as wall bearing depth over the edge beams of the partially bearing solution. So, steel angle is usually used in all the faced long to ensure the required bearing depth (Fig. 6)(Adell Argilés 2003).

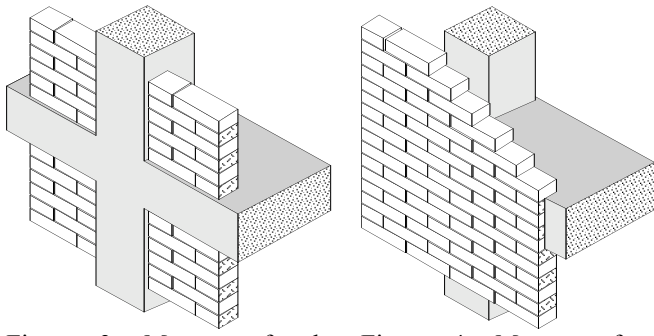


Figure 3: Masonry façade where columns and edge beams are seen.

Figure 4: Masonry façade where columns and edge beams are covered.

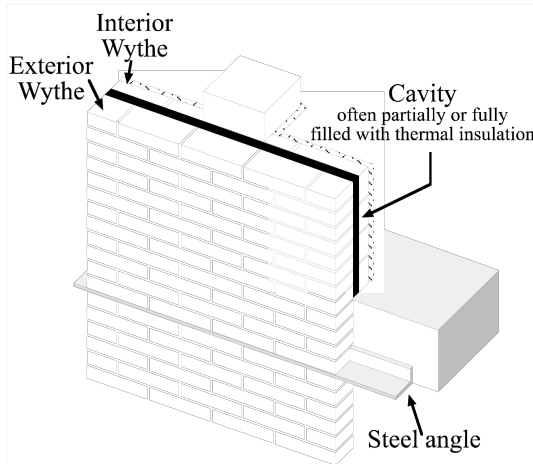


Figure 5: Exterior wythe built out of the plane of the edge beams.

Although the total bearing solution is the best, based on structural considerations, the last two solutions have the advantage of a better appearance and of leading to a larger effective area of the flats, which make these two solutions economically better in spite of their higher initial cost. The partial bearing of the wall is the most used solution in Spain. The masonry units are usually arranged with two thirds of the brick width supported on the edge beam. Dimensions of the customary brick units, Metric and DIN, are shown in figure 7 (Adell Argilés 2003, Hispalyt 1998).

There are no Spanish standards for this construction system. Usually the standards NBE_FL90 (Bearing walls) (Spanish standards 1990), NTE-FFL (External masonry walls of brickwork design) (Spanish Technical standards 1978) and NTE EFL (structural brickwork calculations) (Spanish Technical standards 1977) are used. The first gives instructions about the properties of the mortar and masonry units used in bearing walls and the last two standards provide rules for the structural design of bearing walls. A considerable number of these buildings show cracking in different zones of the façade walls. As a result of the lack of standards, every construction company uses its own experience to prescribe the necessary recommendations to minimize the width and extension of the cracks. There are many possible load patterns that can cause such cracks.

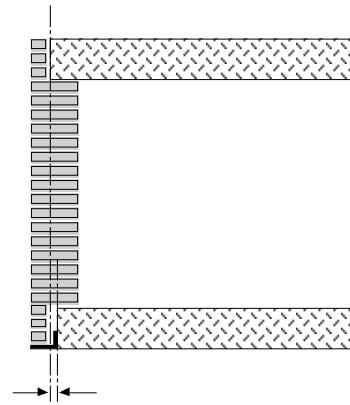


Figure 6: Horizontal gap between the vertical planes of the faces of the edge beams.

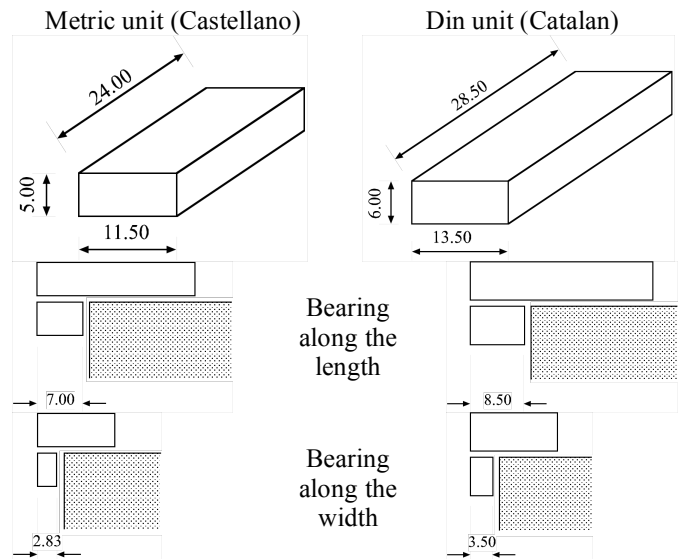


Figure 7: Spanish masonry units (dimensions in cm).

As a large number of flats were constructed in a short period, masonry units might be used before the necessary curing time. Most of the expected expansion in ceramic bricks develops in three or four years, but about 75 percent of it takes place in the first fifteen days after the fabrication (Adell Argilés 2003). The total expansion values and rates depend strongly on the type of the used clays.

Most of these façades were constructed without horizontal expansion joints. The walls are tied to columns with special metallic elements. The joint between the last row of masonry units and the edge beams is totally filled with mortar (Hispalyt 1998). This type of confinement and the volume changes of the masonry units due to water absorption or temperature variations can cause cracking.

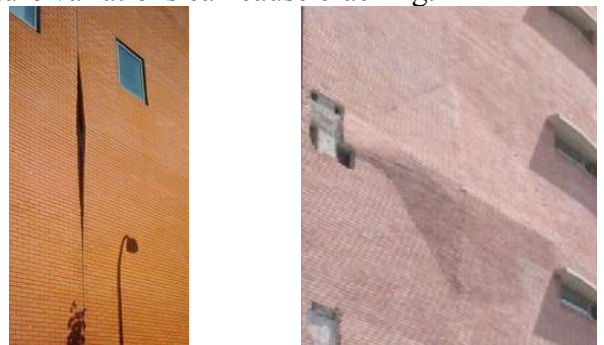


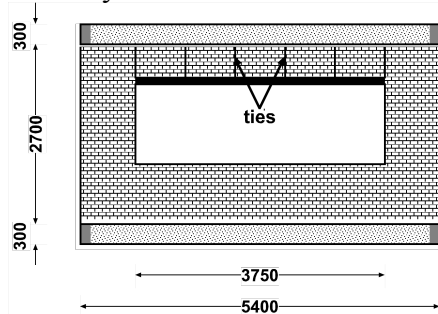
Figure 8: Cracked panels.

Figure 8 shows two cracked panels. Partial bearing of the exterior wythe generates torsion moment on the edge beams. Rotation of edge beams can also cause cracking. In the USA, brick veneer walls are also intensively used, but the wall is totally constructed out of the edge beam plane as shown in figure 5. The difference is that a horizontal expansion joint is left just below the steel angle that holds the wall (Memari et al. 2002, Drysdale et al. 1994).

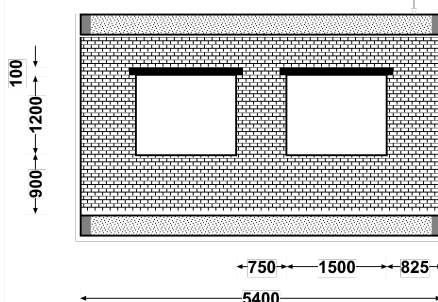
The movement of the building as a result of wind loads is also a possible cause of cracking, especially in the last floor. The authors developed special finite element, based on the strong discontinuity approach and the cohesive crack theory, that is very effective in the numerical simulation of cracking in quasi brittle materials such as concrete and masonry. The authors applied such element to the analysis of the cracks appearing in the foregoing masonry walls in order to have a better understanding of the cracking phenomena.

2 STRATEGY OF THE WORK

As a large number of walls were simulated, a pre-processor program with an easy user interface was developed to automatize the mesh generation process performed mainly using the ANSYS program. The special finite element was implemented in three different programs, i.e. as a user element in FEAP, as a special user material in ABAQUS and finally in an Object Oriented special purpose finite element code. Further details of this element can be found in (Sancho et al. 2004). In the study presently reported, the simulation was performed in two dimensions. The finite element is however capable of three-dimensional analysis.



a. Geometry I: One opening with tied lintel



b. Geometry II: Two openings with bearing lintel

Figure 9: Wall geometries used in the analyses. (All dimensions are in mm).

In this study, a representative panel far from the boundaries of the façade is considered (i.e. it is assumed that there is large number of panels surrounding the studied panel in all directions). In a first series of analyses, a sensitivity analysis was carried out for each geometry to find the best set of computational parameters (such as mesh element density, load increment or calculation tolerance). The corresponding values were then kept constant in the remaining computations.

3 INPUT DATA

3.1 Geometric layout of the studied walls

Two different wall geometries were studied. Figure 9 shows the tested wall geometries. The layout was selected by a consulting office for a large number of construction companies in Spain. The two models have the same external dimensions but the window layout is different. A vertical expansion joint is assumed to exist every two panels. One panel is usually studied when there is a total symmetry. In the last load case two panels were studied, as shown next, because there is no symmetry.

3.2 Load cases

Four different load cases were used as depicted in figure 10. The first case assumes imposed deflection

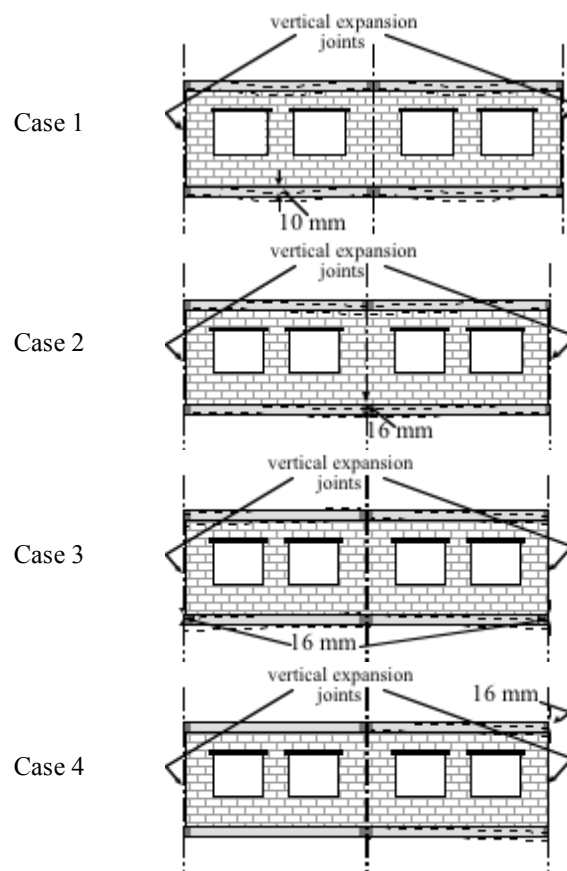


Figure 10: Load cases.

of 10 mm in the mid span of the beams with parabolic distribution. This is equivalent to a uniformly distributed load applied to the beam. The second case assumes a settlement of 16 mm in only one axis of the columns. This axis of columns is in the mid point between the expansion joints. In the third case, the settlement is applied to the two adjacent edges of the expansion joint. The last case is the same as the third but the settlement was applied to only one axis coinciding with an expansion joint.

3.3 *Material properties assumed in the simulation*

Every tested panel has two different materials, steel and bricks. Steel is used for beams, columns, lintel and their ties (in the first geometry). The modulus of elasticity of the steel is taken to be 200 GPa. There are many papers in the literature devoted to the behavior of the masonry units and mortar. Most of those papers deal with concrete blocks. In references (Beall 1993, Alcoser & Klingner 1994) it is shown that the overall strength of the wall depends primarily on the compressive strength of the unit, and very little on the mortar compressive strength. Other analytical papers (Zucchini & Lourenco 2004, Lee et al. 1996, Uva & Salerno 2005) uses the homogenization technique to give relations between the strength of the masonry unit and mortar with the overall strength of the wall. The same concept was investigated experimentally (Khalaf et al. 1994, Ramamurthy et al. 2000). As the masonry wall is a non-homogeneous material, several works investigate the strength of the masonry wall at varying directions with the bed joint (Khatab & Drysdale 1992). From all mentioned papers, it can be concluded that an equivalent homogeneous material can be used for masonry walls. The equivalent strength depends on the strength of the unit and mortar as well as on the direction of the loading with respect to the bed joint where the strength changes by about 20 % (Khatab & Drysdale 1992). So, in this paper, homogenous isotropic material is assumed for the masonry wall with modulus of elasticity of 3 GPa, fracture energy of 100 N/m and tensile strength of 1.0 MPa.

3.4 *Boundary conditions*

For the first case of loading, the column lines coincide with vertical axes of symmetry for both the structure and the brick wall, as shown in figure 10. Therefore, for this case only one panel needs to be analyzed.

In the second and third cases, although there are two axis of symmetry along the two sides of the panel for the wall, there is only one axis of symmetry for the structure, which lies at the mid point between two adjacent expansion joints. The exact boundary conditions of the beams at the ends which coincide the joints is not known exactly because of

the unknown stiffness of the remaining part of the structure at both sides of the panel. To make the calculation faster using the smallest possible number of nodes, one panel was used and two extreme conditions at the end of the beam were considered: In the first boundary conditions, it is assumed that the beams were hinged at one end, and fixed in the second. The exact condition lies in-between these two extreme conditions.

The last case is like the second and third cases with respect to the definition of the boundary conditions of the beams, but the axis of symmetry of the wall coincides with the line of columns on the right. In this case two panels were used. Fixed and hinged ends for the left end of the beams were considered as before.

Geometry I under load case one was used to make the sensitivity analyses to find suitable values for the calculation parameters.

3.5 *Adaptation factor*

To prevent the calculation block, the program permits that cracks with width lesser than $\alpha G_f / f_t$ can change the direction till found the correct one, where G_f is the fracture energy and f_t is the tensile strength. The factor α called adaptation factor Paper (Sancho et al. 2005a) shows that a value of 0.2 for the adaptation factor is sufficient for no blocking the calculation. This value is used in all the calculations.

4 RESULTS

4.1 *Geometry I, load case 1*

Triangular elements were used to mesh the wall and special elements with embedded crack were used for calculation. Quadratic four-node elements were used to mesh the beams and the lintel. Enhanced-strain quadrilateral elements developed by J. Simo and R.L. Taylor were used for the computations, since this type of element allows computing the stress and strain in bending accurately with few elements across the beam depth.

Figure 11 shows the resulting crack pattern for a deflection of 10 mm for a computation carried out at loading steps of 0.1 mm, with a tolerance of 1e-6 and a mesh size corresponding to 2100 elements. Black and grey crack lines correspond to crack openings respectively larger and lesser than 0.02 mm (corresponding to adaptation factor $\alpha = 0.2$ (Sancho et al. 2005a)). The wall appears to be extensively cracked for a deflection at mid-span of 10 mm; therefore in subsequent computations the mid-span deflection was reduced to 2.5 mm.

To increase the accuracy, the deflection step was reduced to 0.01 mm. The resulting crack pattern is shown in the upper plot in figure 12. Next, to de-

crease the time of computation, the beams surrounding the concrete were eliminated and the parabolic vertical displacements were applied directly to the upper and lower edges of the masonry panel. The resulting crack distribution (lower plot in Fig. 12) was clearly different from the previous one, which demonstrates that the two ways of applying the boundary conditions are not equivalent and that the results are sensitive to the computational details. Moreover, the time required for the last type of computation was longer than for the one involving the beams, despite that the number of degrees of freedom were less, which is counter-intuitive.

Four possible sources for the observed differences were identified:

- 1 The meshes used for the masonry are very similar, but not identical
- 2 The horizontal displacements at the upper and lower edge of the masonry panel are not the same (in the second case the horizontal displacement is zero)
- 3 The results are sensitive to the tolerance
- 4 The results are sensitive to the step size.

Figure 13 shows that the positions of the nodes for the two cases in figure 12 are actually very close. However, to fully avoid this problem, in all subsequent computations, the beam and wall are always meshed and then the beams are removed.

To appropriately account for the horizontal displacements along the upper and lower edges of the masonry, the horizontal displacement of the lower and upper edges of the beams were computed using classical beam theory and Navier's hypothesis for the cross-section of the beams. Figure 14 shows the horizontal and vertical components of the displacement at the upper and lower edges of the panel. Figure 15 shows that with this condition, the results are identical for computations with and without explicit inclusion of the beams.

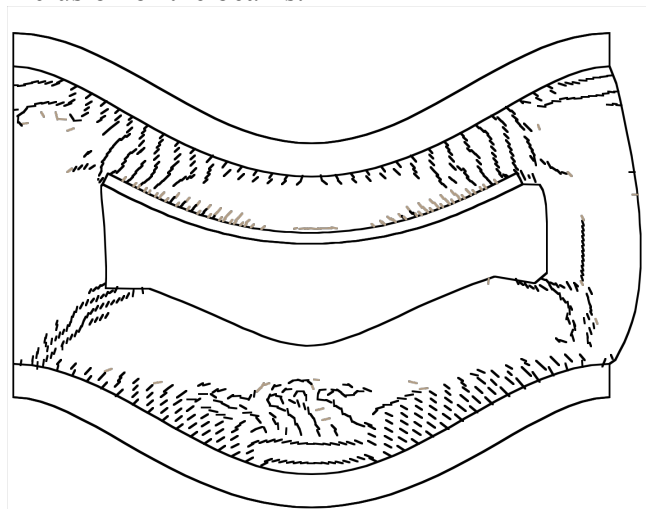
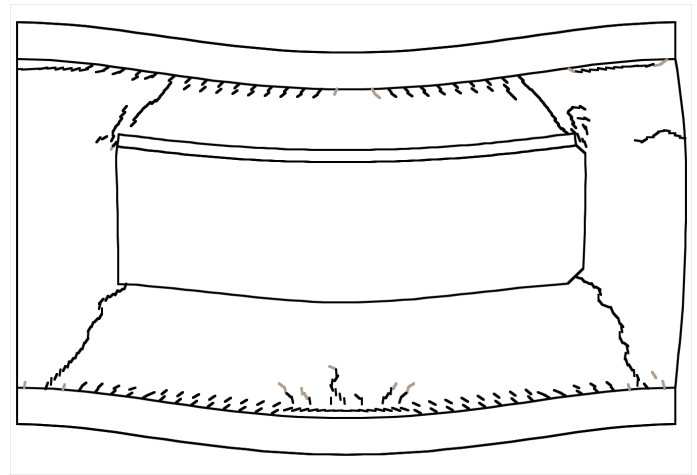
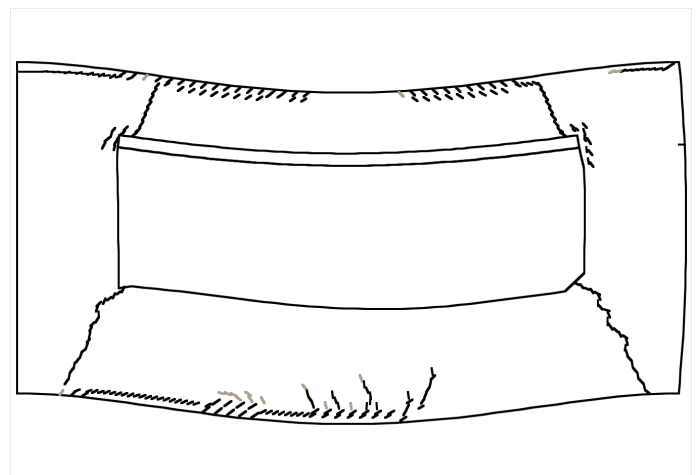


Figure 11: Crack pattern for geometry I, load case 1. (maximum deflection = 10 mm, deflection increment = 0.1 mm, Tolerance = $1e-6$) Black and grey crack lines correspond to crack openings respectively larger and lesser than 0.02 mm.



a. Explicit modeling of edge beams



b. Implicit computed boundary conditions

Figure 12: Crack pattern with and without edge beams. (max. deflection = 2.5 mm, deflection increment = 0.01 mm, Tol. = $1e-6$)

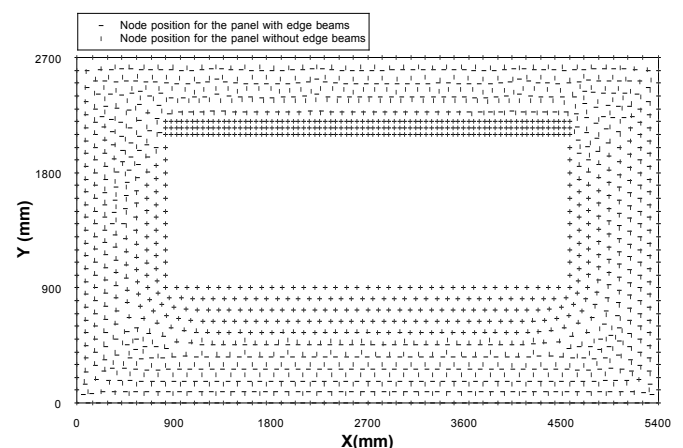


Figure 13: Node layout for computations with explicit modeling of edge beams and without beams. X, Y is horizontal and vertical distances to the bottom-left corner of the masonry panel.

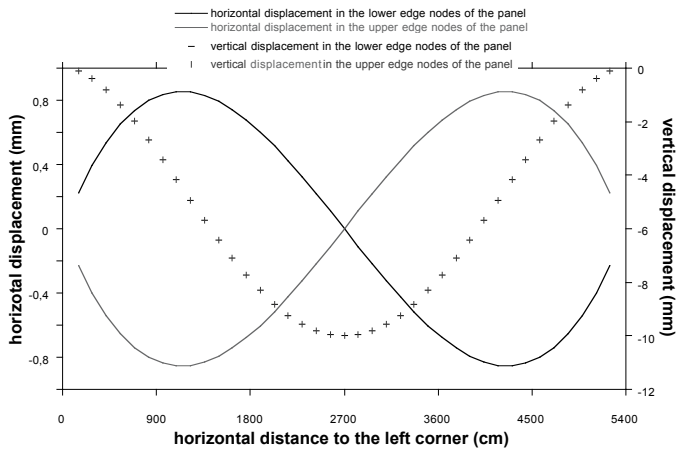


Figure 14: Computed horizontal and vertical displacements at the top and bottom edges of the masonry panel (according to the assumed deflection of the edge beams).

The influence of the step size is shown in figure 15. The results are essentially identical for step sizes equal or less than 0.01 mm, and thus the step size was set to that value in all subsequent calculations.

When reducing the tolerance down to $1e-12$, the time of computation of the panels without the beams was less than those with the beams, as expected. The explanation for this behavior is that, in the panel with beams, the stiffness of the concrete is much larger than that of the masonry and thus the unbalance of nodal forces at the beginning of the step is larger, which means that identical relative tolerances (as used) correspond to larger absolute tolerances for the panel with beams.

Following this analysis, in the remaining of the research masonry panels with imposed parabolic displacements including computed horizontal components, with a step size of 0.01 mm and a tolerance of $1e-12$ were used.

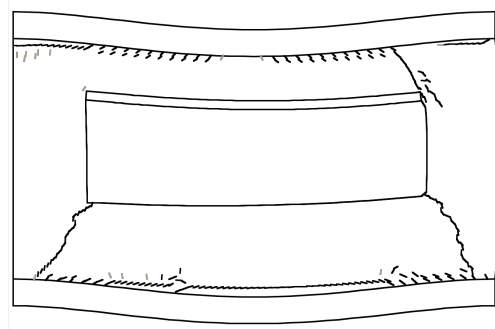
4.2 Geometry II, load case 1

Applying the load case 1 to the geometry II in figure 9 with the calculation parameters defined before, the results shown in figure 16 are obtained.

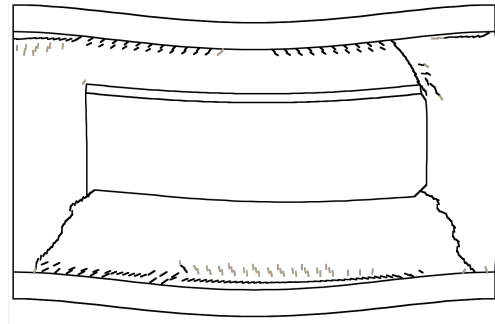
Figure 15 shows that for geometry I the dominant crack is the horizontal crack at the bottom of the masonry, while figure 16 for the geometry II shows that this type of crack doesn't appear because of the compressive strut connecting the bottom and top strips. A vertical crack appears in the middle-upper part that is not present in geometry I. However, the most open cracks are the bottom-left and bottom-right cracks at the window corners.

4.3 Load case 2, 3 and 4

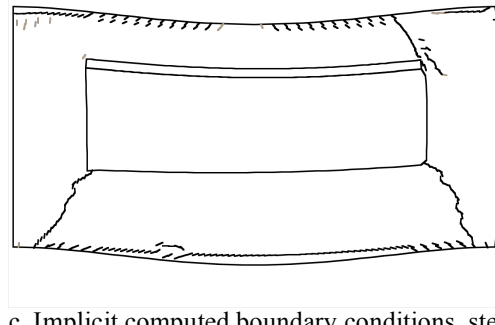
Computations were carried out to ascertain the cracking behavior of geometries I and II under loadings 2-4. Since the crack patterns were very similar for both geometries, only results for geometry I are given here (Figs. 17, 18 & 19).



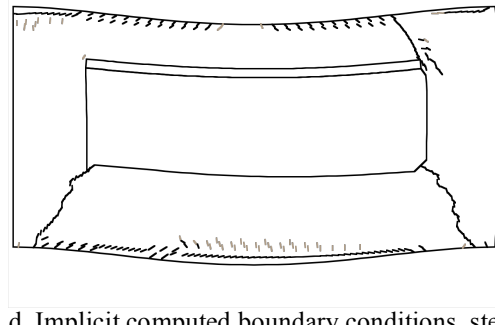
a. Explicit modeling of edge beams, step inc. = 0.01.



b. Explicit modeling of edge beams, step inc. = 0.002.



c. Implicit computed boundary conditions, step inc. = 0.01.



d. Implicit computed boundary conditions, step inc. = 0.002.

Figure 15: Crack patterns for Geometry I under load case 1. The maximum deflection is 2.0 mm and the tolerance is $1e-12$ in all cases.

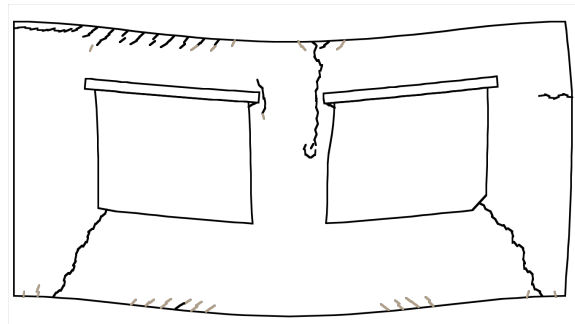


Figure 16: Crack pattern for Geometry II under load case 1. (Maximum deflection 2.0 mm, step increment 0.002 mm, tolerance $1e-12$.)

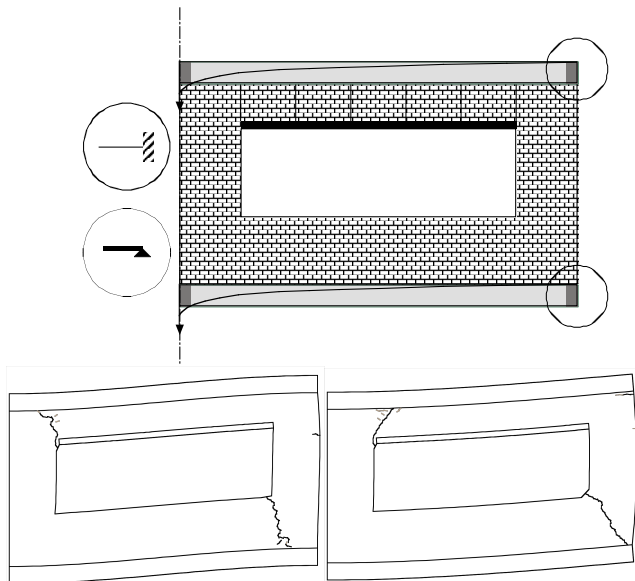


Figure 17: Crack pattern for Geometry I under load case 2

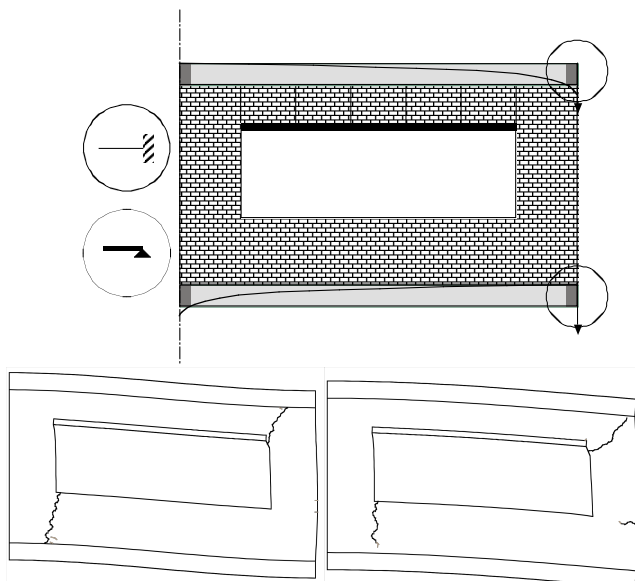


Figure 18: Crack pattern for Geometry I under load case 3.

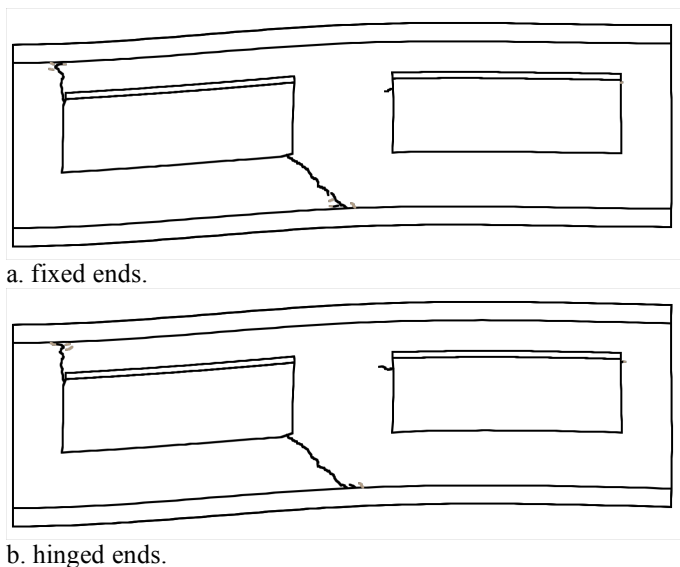


Figure 19: Crack pattern for Geometry I under load case 4.

Figure 17 & 18 show the results for load case 2 and load case 3 respectively (As previously explained, two extreme boundary condition were assumed at the end opposite to the one experiencing the settlement: fixed end (left) or hinged end (right). As can be seen, two diagonally opposed cracks at the window corner appear in all cases, and the exact boundary conditions influence only slightly the direction of the crack path.

Figure 19 shows the results for loading case 4. As in the previous cases, two extreme boundary conditions were assumed: fixed ends (top) and hinged ends (bottom). The results are nearly identical in this case and similar to those in the loading cases 2 and 3.

5 CONCLUSIONS

From the foregoing results, the foregoing conclusions may be drawn

- 1 Finite elements with embedded cohesive cracks can describe the relative complex cracking patterns that arise in masonry façades, with multiple cracks growing simultaneously. As described elsewhere, this kind of elements can be essentially implemented in a general-purpose finite element code.
- 2 Careful fitting of computation parameters is required to achieve consistent results. A simple methodology to do so is outlined in this paper.
- 3 The influence of the geometry on the crack pattern is substantial only for load case 1 (excessive deflection of the beams). The remaining cases 2-4 (settlement of supports) lead to similar crack patterns.
- 4 For the deflections or settlements in the range $1/500$ to $1/300$ of the span (in the first intent of geometry one loaded with case one), the masonry appears to be fully cracked with crack openings of the same order of magnitude as the beam deflections.
- 5 Although the results shown correspond to a particular set of material properties for the masonry, the final crack pattern is similar for any set of realistic material properties (crack initiation may change, but the final cracks are essentially the same)
- 6 Since allowed design values for deflections or settlements is usually in the range $1/500$ to $1/300$ of the span, the foregoing results implicate that the real deflections or settlements are actually much less than the design values in most buildings, since the occurrence of pathological cracking such as that in figures 14-17 is, fortunately, scarce (for the case of totally bearing panels).

6 FUTURE WORK

- 1 This suggests that a large scale experimental monitoring plan of actual settlements and deflections would be essential to correlate design values and actual values for deflections.
- 2 Further experimental work on masonry panels in actual buildings (rather than laboratory-made panels) would be required to ascertain average and statistical properties of masonry façades
- 3 The 2D computations must be complemented with 3D analysis to properly take into account the effect of eccentric loading due to partial support of the masonry on the panels. Such extension is currently being carried out (Sancho et al. 2005b).

7 ACKNOWLEDGMENTS:

The authors gratefully acknowledge support for this research from the Spanish Ministry of Education under Grant CIT 380000-2005-40, and from the Comunidad de Madrid under Project S-0505/MAT-00155 (DUMEINPA).

REFERENCES:

- Adell Argilés, J. M. 2003. *Tratado De Construcción, Fachadas y Cubiertas*. Madrid, Spain: Editorial Munilla-Leria.
- Alcoser, S.M. & Klingner, R.E. 1994. Masonry Reserch in Americas. *ACI SP-147-05, September*: 127-169.
- Beall, C. 1993. *Masonry design and detailing for Architects Engineers, and Constructors*. Third edition, McGraw-Hill.
- Casabbone, C. 1994. General Description of Systems and Construction Practices. *ACI SP-147-02, September*: 21-55.
- Drysdale, R.G. Hamid, A.A. & Baker, 1994. *Masonry Structure, Behavior and Design*. New Jersey, USA: Prentice-Hall.
- Gallegos, H. 1994. Masonry in Peru. *ACI SP-147-11, September*: 307-331.
- Garcia, L.E. & Yamin, L.E. 1994. A Review of Masonry Construction in Colombia. *ACI SP-147-10, September*: 283-305.
- Hispalayt, 1998. *Ejecución de fachadas con ladrillo cara vista*. Manual, Madrid, Spain: Editorial la sección de Ladrillo de Cara Vista de Hispalayt.
- Khalaf, F.M. Hendy, A.W. & Fairbairn, D.R. 1994. Study of the Compressive Strength of Blockwork Masonry. *ACI Structural Journal, Vol. 91, No. 4, July-August*: 367-375.
- Khattab, M.M. & Drysdle, R.G. 1992. Tests of Concrete Block Masonry Under Biaxial Tension-Compression. *Canadian Masonry Symposium, 15-17 June (1992)*: 645-656.
- Lee, J.S. Pande, G.N. MIddIeton, T.J. & Kralj, B. 1996. Numerical Modeling Of Brick Masonry Panels Subject To Lateral Loadings. *Computers and Structures, Vol. 61*: 735-745. Great Britain.
- Meli, R. & Garcia, L.E. 1994. Structural Design of Masonry Buildings: The Mexican Practice. *ACI SP-147-08, September*: 239-262.
- Memari, A.M. Burnet, E.F.P. & Brian, M.K. 2002. Seismic response of a new type of masonry tie used in brick veneer walls. *Construction and Building Materials, 6*: 397 - 407.
- Ramamurthy, K., Sathish, V. & Ambalavanan, R. 2000. Compressive Strength Prediction of Hollow Concrete Block Masonry Prisms. *ACI Structural Journal, Vol. 97, No. 1, January-February*: 61-67.
- Sancho, J.M. Planas, J. Cendón, D.A. Reyes, E. & Gálvez, J.C. 2007. An embedded cohesive crack model for finite element analysis of concrete fracture. *Engineering Fracture Mechanics, Vol. 74*: 75-86.
- Sancho, J.M. Planas, J. Cendón, D.A. Gálvez, J.C. & Reyes, E. 2005. Ventajas De La Fisura Cohesiva Adaptable En La Simulación Numérica De La Fractura De Materiales Cuasi-frágiles. *Anales de Mecánica de la Fractura, Vol. 22*: 553-558.
- Sancho, J.M. Planas, J. Fathy, A.M. Gálvez, J.C & Cendón, D.A. 2006. Three-dimensional simulation of concrete fracture using embedded crack elements without enforcing crack path continuity. *Int. J. Numer. Anal. Meth. Geomech.* in press, published online, September 4, 2006.
- Spanish standards for bearing walls, 1990. *Muros resistentes de fábrica de ladrillo*. NBE FL-90.
- Spanish Technical standards for buildings, 1977. *Structural brickwork calculations*. NTE-EFL.
- Spanish Tecnical standards for buildings, 1978. *External masonry walls of brickwork design*. NTE-FFL.
- Uva, G. & Salerno, P.B.G. 2005. Towards a multiscale analysis of periodic masonry brickwork: A FEM algorithm with damage and friction. *Solids and Structures, in press, received 2 June (2005)*.
- Yamin, L.E. & Garcia, L.E. 1994. Masonry Materials. *ACI SP-147-01, September*: 1-20.
- Zucchini, A. & Lourenco, P.B. 2004. A coupled homogenisation-damage model for masonry cracking. *Computers and Structures, 82*: 917-929. Great Britain.